Journal of Applied Mathematics and Physics, 2023, 11, 3042-3060
https://www.scirp.org/journal/jamp
ISSN Online: 2327-4379
ISSN Print: 2327-4352

Solitons and Bifurcations for the Generalized Tzitzéica Type Equation in Nonlinear Fiber Optics

Xujie Jiang

College of Mathematics and Information Science, Nanchang Hangkong University, Nanchang, China
Email: jmq991209@sina.com

How to cite this paper: Jiang, X.J. (2023) Solitons and Bifurcations for the Generalized Tzitzéica Type Equation in Nonlinear Fiber Optics. *Journal of Applied Mathematics and Physics*, **11**, 3042-3060.
https://doi.org/10.4236/jamp.2023.1110201

Received: September 18, 2023
Accepted: October 27, 2023
Published: October 30, 2023

Abstract

Solitons and bifurcations for the generalized Tzitzéica type equation are studied by using the theory of dynamical systems and Hamilton function. With the help of Maple and bifurcation theory of differential equations, the bifurcation parameter conditions and all the bifurcation phase portraits are obtained. Because the same energy value of the Hamiltonian function is corresponding to the same orbit, thus the periodic wave solutions, bright soliton and dark soliton solutions are defined.

Keywords

Generalized Tzitzéica Type Equation, Homoclinic Orbit, Periodic Wave Solution, Bright Soliton, Dark Soliton

1. Introduction

The Tzitzéica type equations contain the following four nonlinear evolution equations [1]-[6]

$$u_{xx} - u_{tt} + \mathrm{e}^{u} - \mathrm{e}^{-2u} = 0, \tag{1.1}$$

and

$$u_{xt} + \mathrm{e}^{u} = 0, \tag{1.2}$$

and

$$u_{xt} + \mathrm{e}^{u} + \mathrm{e}^{-2u} = 0, \tag{1.3}$$

and

$$u_{xt} - \mathrm{e}^{-u} - \mathrm{e}^{-2u} = 0. \tag{1.4}$$

which play an important role in nonlinear fiber optics. Equations (1.1), (1.2), (1.3) and (1.4) present the Tzitzéica, Liouville, Dodd-Bullough-Mikhailov and Tzitzéica-Dodd-Bullough equations, respectively. For instance, Kumar [1] studied the Tzitzéica type equations by the method of sine-Gordon expansion. In [7], with the help of generalized exponential rational function method, the authors researched Equations (1.1) and (1.4). Zafar [8] discussed Equations (1.1), (1.3) and (1.4) by the Painlevé transformation and the simplest equation method. Hosseini [9] studied the Tzitzéica type equations using the $\exp_a$ function method. In [10], the $\left(\frac{G'}{G}\right)$-expansion method was applied for constructing more general exact solutions of the Tzitzéica type equations. In [11], the improved $\tan\left(\frac{\phi(\xi)}{2}\right)$-expansion method was used to study the Tzitzéica type equations and the dispersive dark optical solitons were obtained. For more literature, we can refer to [12]-[19].

Obviously, there is no single way to solve the soliton solutions of all nonlinear evolution equations, which leads to the generation of many new methods, such as the G'/G^2-expansion method and the sine-cosine method [20], the functional variable method and first integral approach [21], the semi-inverse variational principle [22], Lie symmetry approach [23], the method of F-expansion [24] [25], the modified simple equation method and the trial equation method [26] [27], the asymmetric method [28], the Gaussian ansatz [29] [30], the soliton perturbation theory [31] [32], the simplest equation method and the G'/G-expansion method [33] [34], the theory of dynamical systems [35] [36] [37] [38].

In this paper, We will devote ourselves to research the following generalized Tzitzéica type equation

$$\kappa u_{tt} - \kappa u_{xx} + \alpha u_{xt} + \beta e^{u} + \gamma e^{-u} + \eta e^{-2u} = 0, \tag{1.5}$$

where α, β, γ and η are real constants. As far as we know, Equation (1.5) has not been studied. In particular, we notice that some well-known equations are included in Equation (1.5). When $\kappa = 1$, $\alpha = \gamma = 0$, $\beta = -1$ and $\eta = 1$, Equation (1.5) reduces to the Tzitzéica equation. When $\kappa = \gamma = \eta = 0$ and $\alpha = \beta = 1$, Equation (1.5) reduces to the Liouville equation. When $\kappa = \gamma = 0$ and $\alpha = \beta = \eta = 1$, Equation (1.5) reduces to the Dodd-Bullough-Mikhailov equation. When $\kappa = \beta = 0$, $\alpha = 1$ and $\gamma = \eta = -1$, Equation (1.5) reduces to the Tzitzéica-Dodd-Bullough equation. Using the theory of dynamical systems, the bounded solitons and bifurcations of Equation (1.5) will be discussed. These conclusions are new and have important applications in mathematics and physics. It can help us understand many experiments in physics, and can reveal the laws of motion and the objective nature of physical experiments.

2. Traveling Wave Transformation and First Integral

Introducing the following function transformation

$$u(x,t)=\ln(v(x,t)), \tag{2.1}$$

where $v(x,t)>0$. Without loss of generality, we only discuss the traveling wave solutions when $v(x,t)>0$.

Substituting Equation (2.1) into Equation (1.5), we get

$$\kappa vv_{tt}-\kappa vv_{xx}+\alpha vv_{xt}+\kappa\left(v_t^2+v_x^2\right)-\alpha v_x v_t+\beta v^3+\gamma v+\eta=0. \tag{2.2}$$

In order to seek traveling wave solutions of Equation (2.2), we assume that

$$v(x,t)=v(\xi),\quad \xi=x-ct, \tag{2.3}$$

where c is the wave speed. Substituting Equation (2.3) into Equation (2.2), we get

$$\left(\kappa c^2-\kappa-\alpha c\right)\left[v(\xi)\frac{\mathrm{d}^2v(\xi)}{\mathrm{d}\xi^2}-\left(\frac{\mathrm{d}v(\xi)}{\mathrm{d}\xi}\right)^2\right]+\beta v(\xi)^3+\gamma v(\xi)+\eta=0. \tag{2.4}$$

Let $\frac{\mathrm{d}v(\xi)}{\mathrm{d}\xi}=y(\xi)$, then Equation (2.4) is equivalent to the following two dimensional singular traveling wave system

$$\begin{aligned}&\frac{\mathrm{d}v(\xi)}{\mathrm{d}\xi}=y(\xi),\\&\frac{\mathrm{d}y(\xi)}{\mathrm{d}\xi}=\frac{y(\xi)^2+\alpha_1v(\xi)^3+\alpha_2v(\xi)+\alpha_3}{v(\xi)},\end{aligned} \tag{2.5}$$

where $\alpha_1=\frac{\beta}{\alpha c+\kappa-c^2\kappa}$, $\alpha_2=\frac{\gamma}{\alpha c+\kappa-c^2\kappa}$, $\alpha_3=\frac{\eta}{\alpha c+\kappa-c^2\kappa}$.

System (2.5) has the following Hamilton function

$$H(v,y)=\frac{y^2}{v^2}-\frac{2v^3\alpha_1-2v\alpha_2-\alpha_3}{v^2}=h, \tag{2.6}$$

where h is a real constant.

3. Bifurcation of Parameters and Phase Portraits

Firstly, we study the following associated regular system of system (2.5)

$$\begin{aligned}&\frac{\mathrm{d}v(\zeta)}{\mathrm{d}\zeta}=v(\zeta)y(\zeta),\\&\frac{\mathrm{d}y(\zeta)}{\mathrm{d}\zeta}=y(\zeta)^2+\alpha_1v(\zeta)^3+\alpha_2v(\zeta)+\alpha_3,\end{aligned} \tag{3.1}$$

where $\mathrm{d}\xi=v\mathrm{d}\zeta$. System (2.5) and system (3.1) have the same Hamiltonian function. Consequently, system (2.5) and system (3.1) have the same dynamic properties except for the straight line $v=0$. Near the straight line $v=0$, the dynamics of the solutions for system (2.5) usually change abruptly.

Define

$$f(v)=\alpha_1v^3+\alpha_2v+\alpha_3,\quad v_1=-\sqrt{-\frac{\alpha_2}{3\alpha_1}},\quad v_2=\sqrt{-\frac{\alpha_2}{3\alpha_1}}.$$

Discussing the equilibrium points of the system (3.1), we get the following proposition.

Proposition 3.1

(i) When $\alpha_1 = 0$, there exists a equilibrium point $\left(-\frac{\alpha_3}{\alpha_2}, 0\right)$ on the *v-axis*.

(ii) When $\alpha_1\alpha_2 > 0$, $f(v)$ is a monotone function. Therefore there is only one equilibrium point on the *v-axis*.

(iii) When $\alpha_1\alpha_2 < 0$, $f(v_1)f(v_2) > 0$, there is one equilibrium point on the *v-axis*.

(iv) When $\alpha_1\alpha_2 < 0$, $f(v_1)f(v_2) < 0$, there exist three different equilibrium points on the *v-axis*.

(v) When $\alpha_1\alpha_2 < 0$ and $f(v_1)f(v_2) = 0$, there exist two equilibrium points on the *v-axis*, one of which is a double equilibrium point.

(vi) When $\alpha_2 = 0$, $\alpha_3 = 0$, there is a triple equilibrium point $(0,0)$ on the *v-axis*.

(vii) When $\alpha_2 = 0$, $\alpha_3 \neq 0$, there is a equilibrium point $\left(\sqrt[3]{-\frac{\alpha_3}{\alpha_1}}, 0\right)$ on the *v-axis*.

(vii) When $a_3 < 0$, there are two equilibrium points $\left(0, \pm\sqrt{-\alpha_3}\right)$ on the *y-axis*. When $a_3 > 0$, there is no equilibrium point on the *y-axis*. When $a_3 = 0$, there is a double equilibrium point $(0,0)$ on the *y-axis*.

Suppose $J(v,y)$ is the Jacobian matrix of the linearized system (3.1) and defines

$$J(v,y) = \begin{bmatrix} y & v \\ 3\alpha_1 v^2 + \alpha_2 & 2y \end{bmatrix}. \tag{3.2}$$

From (3.2), we know that

$$det\,J(v,0) = -3\alpha_1 v\left(v^2 + \frac{\alpha_2}{3\alpha_1}\right) = -3\alpha_1 v(v - v_1)(v - v_2).$$

According to the above analysis, the parameter condition $\frac{\alpha_2}{\alpha_1} = -\frac{27}{4}\left(\frac{\alpha_3}{\alpha_2}\right)^2$ is obtained from $f(v_i) = 0$, $i = 1,2$. Let $k_1 = \frac{\alpha_2}{\alpha_1}$, $k_2 = \frac{\alpha_3}{\alpha_2}$. Thus there are three bifurcation curves $L_1 : k_1 = 0$, $L_2 : k_2 = 0$ and $L_3 : k_1 = -\frac{27}{4}k_2^2$ in the (k_1, k_2) -parameter plane, as shown in **Figure 1**. Using the bifurcation theory of differential equation [35] [36] [37] [38], we obtain the phase portraits of system (2.5), as shown in **Figure 2**.

4. Exact Traveling Wave Solutions of Equation (2.4)

In this section, we will use (2.6) and the Maple software to obtain the bounded traveling wave solutions of Equation (2.4). According to the relationship between

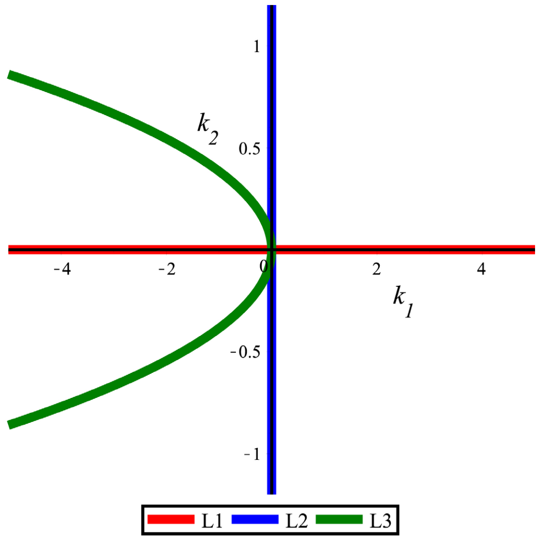

Figure 1. The parameter regions partitioned by bifurcation curves in the (k_1, k_2)-plane.

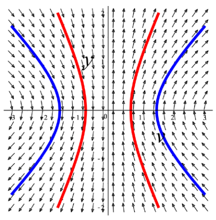

(1) $\alpha_1 = \alpha_2 = 0, \alpha_3 > 0.$

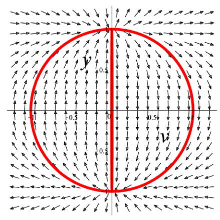

(2) $\alpha_1 = \alpha_2 = 0, \alpha_3 < 0.$

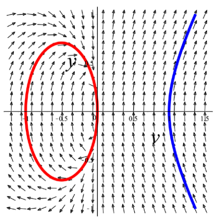

(3) $\alpha_1 = \alpha_3 = 0, \alpha_2 > 0.$

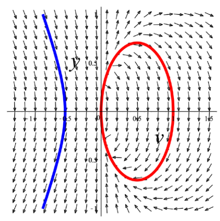

(4) $\alpha_1 = \alpha_3 = 0, \alpha_2 < 0.$

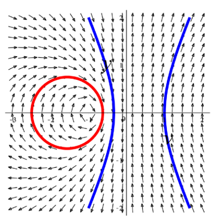

(5) $\alpha_1 = 0, \alpha_2 > 0, \alpha_3 > 0.$

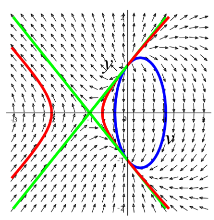

(6) $\alpha_1 = 0, \alpha_2 < 0, \alpha_3 < 0.$

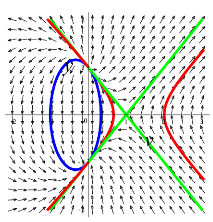

(7) $\alpha_1 = 0, \alpha_2 > 0, \alpha_3 < 0.$

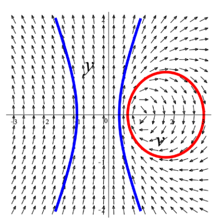

(8) $\alpha_1 = 0, \alpha_2 < 0, \alpha_3 > 0.$

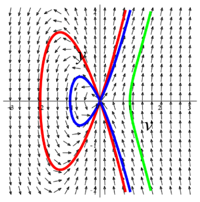

(9) $\alpha_1 > 0, \alpha_2 = 0, \alpha_3 = 0.$

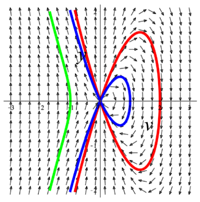

(10) $\alpha_1 < 0, \alpha_2 = 0, \alpha_3 = 0.$

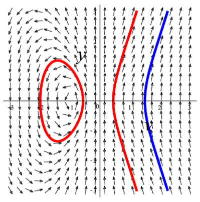

(11) $\alpha_1 > 0, \alpha_2 = 0, \alpha_3 > 0.$

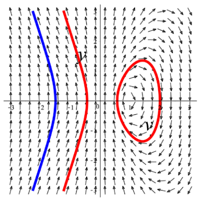

(12) $\alpha_1 < 0, \alpha_2 = 0, \alpha_3 > 0.$

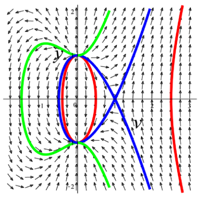

(13) $\alpha_1 > 0, \alpha_2 = 0, \alpha_3 < 0.$

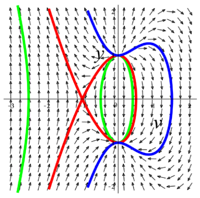

(14) $\alpha_1 < 0, \alpha_2 = 0, \alpha_3 < 0.$

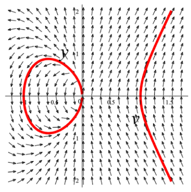

(15) $\alpha_1 > 0, \alpha_2 > 0, \alpha_3 = 0.$

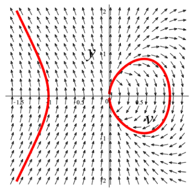

(16) $\alpha_1 < 0, \alpha_2 < 0, \alpha_3 = 0.$

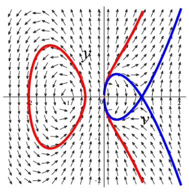

(17) $\alpha_1 > 0, \alpha_2 < 0, \alpha_3 = 0.$

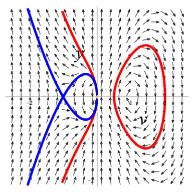

(18) $\alpha_1 < 0, \alpha_2 > 0, \alpha_3 = 0.$

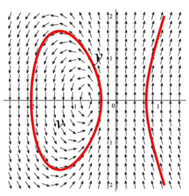

(19) $\alpha_1 > 0, \alpha_2 > 0, \alpha_3 > 0.$

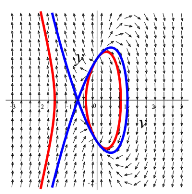

(20) $\alpha_1 < 0, \alpha_2 < 0, \alpha_3 < 0.$

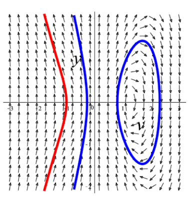

(21) $\alpha_1 < 0, \alpha_2 > 0, \frac{\alpha_3}{\alpha_2} > \sqrt{-\frac{4\alpha_2}{27\alpha_1}}.$

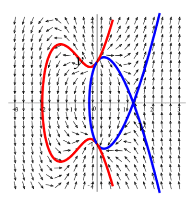

(22) $\alpha_1 > 0, \alpha_2 < 0, \frac{\alpha_3}{\alpha_2} > \sqrt{-\frac{4\alpha_2}{27\alpha_1}}.$

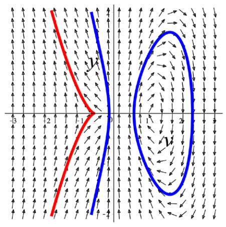

(23) $\alpha_1 < 0, \alpha_2 > 0, \frac{\alpha_3}{\alpha_2} = \sqrt{-\frac{4\alpha_2}{27\alpha_1}}$.

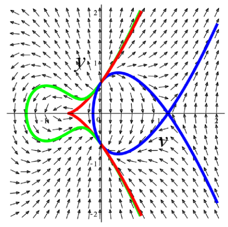

(24) $\alpha_1 > 0, \alpha_2 < 0, \frac{\alpha_3}{\alpha_2} = \sqrt{-\frac{4\alpha_2}{27\alpha_1}}$.

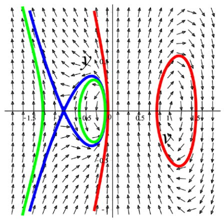

(25) $\alpha_1 < 0, \alpha_2 > 0, 0 < \frac{\alpha_3}{\alpha_2} < \sqrt{-\frac{4\alpha_2}{27\alpha_1}}$.

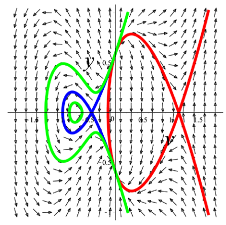

(26) $\alpha_1 > 0, \alpha_2 < 0, 0 < \frac{\alpha_3}{\alpha_2} < \sqrt{-\frac{4\alpha_2}{27\alpha_1}}$.

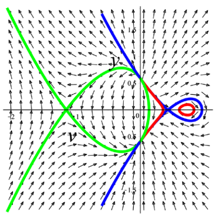

(27) $\alpha_1 < 0, \alpha_2 > 0, -\sqrt{-\frac{4\alpha_2}{27\alpha_1}} < \frac{\alpha_3}{\alpha_2} < 0$.

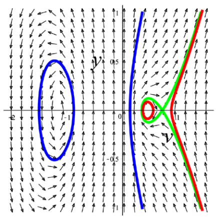

(28) $\alpha_1 > 0, \alpha_2 < 0, -\sqrt{-\frac{4\alpha_2}{27\alpha_1}} < \frac{\alpha_3}{\alpha_2} < 0$.

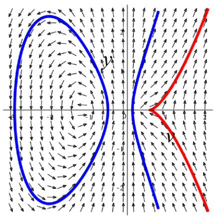

(29) $\alpha_1 > 0, \alpha_2 < 0, \frac{\alpha_3}{\alpha_2} = -\sqrt{-\frac{4\alpha_2}{27\alpha_1}}$.

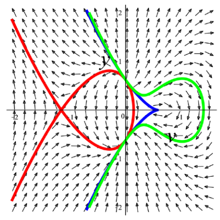

(30) $\alpha_1 < 0, \alpha_2 > 0, \frac{\alpha_3}{\alpha_2} = -\sqrt{-\frac{4\alpha_2}{27\alpha_1}}$.

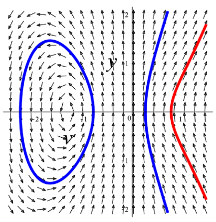

(31) $\alpha_1 > 0, \alpha_2 < 0, \frac{\alpha_3}{\alpha_2} < -\sqrt{-\frac{4\alpha_2}{27\alpha_1}}$.

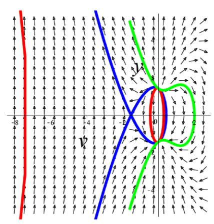

(32) $\alpha_1 < 0, \alpha_2 > 0, \frac{\alpha_3}{\alpha_2} < -\sqrt{-\frac{4\alpha_2}{27\alpha_1}}$.

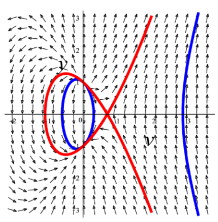

(33) $\alpha_1 > 0, \alpha_2 > 0, \alpha_3 < 0$.

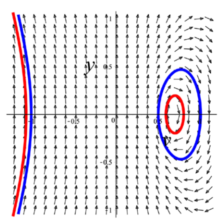

(34) $\alpha_1 < 0, \alpha_2 < 0, \alpha_3 > 0$.

Figure 2. Bifurcations of phase portraits of system (2.5).

the solutions of Equation (1.5) and Equation (2.4), we know that $u(x,t)=\ln(v(x,t))$. Thus we can obtain traveling wave solutions of Equation (1.5). We agree to take only the part of $v(x,t)>0$ as the solutions of Equation (2.4), and we will not repeat it.

From (2.6), we obtain

$$y^2=2v^3\alpha_1+hv^2-2v\alpha_2-\alpha_3. \tag{4.1}$$

Substituting into the first equation of system (2.5), we get

$$\xi=\int\frac{1}{\sqrt{2v^3\alpha_1+hv^2-2v\alpha_2-\alpha_3}}\mathrm{d}v. \tag{4.2}$$

(i) When $\alpha_1=\alpha_2=0$, $\alpha_3<0$, corresponding to **Figure 2(2)**. When $h<0$, there exist a family of periodic orbits defined by $H(v,y)=h$. From Equation (4.2), we obtain

$$\sqrt{-h}\xi=\int_v^{\sqrt{\frac{\alpha_3}{h}}}\sqrt{\frac{1}{\frac{\alpha_3}{h}-s^2}}\mathrm{d}s. \tag{4.3}$$

Thus we get the following solutions, as shown in **Figure 3** and **Figure 4**.

$$v(\xi)=\sqrt{\frac{\alpha_3}{h}}\sin\left(\sqrt{-h}\xi\right), \tag{4.4}$$

and

$$u(x,t)=\ln\left(\sqrt{\frac{\alpha_3}{h}}\sin\left(\sqrt{-h}(x-ct)\right)\right). \tag{4.5}$$

(ii) When $\alpha_1=\alpha_3=0$, $\alpha_2<0$, corresponding to **Figure 2(4)**. When $h<0$, the curves defined by $H(v,y)=h$ are a family of periodic orbits. From Equation (4.2), it follows

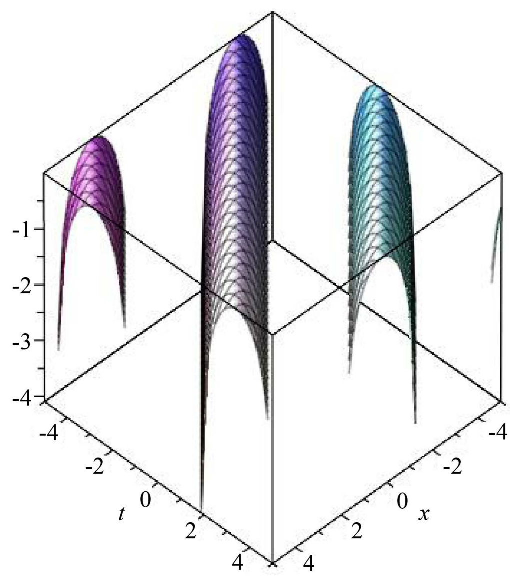

Figure 3. The 3D plot of (4.5).

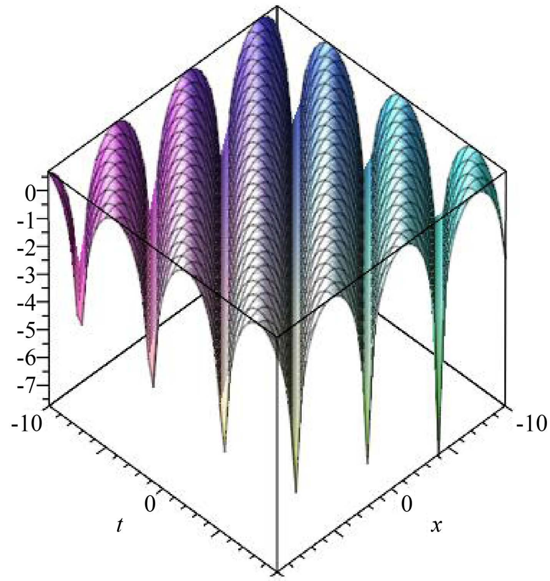

Figure 4. The 3D plot of (4.8).

$$\sqrt{-h}\xi = \int_v^{\sqrt{\frac{2\alpha_2}{h}}} \sqrt{\frac{1}{-s^2 + \frac{2\alpha_2}{h} s}} \mathrm{ds}. \tag{4.6}$$

From Equation (4.6), we get the parameter expressions for $v(\xi)$ and $u(x,t)$ as follows

$$v(\xi) = \frac{\alpha_2}{h} + \frac{\alpha_2}{h} \sin\left(\sqrt{-h}\xi\right), \tag{4.7}$$

and

$$u(x,t) = \ln\left(\frac{\alpha_2}{h} + \frac{\alpha_2}{h} \sin\left(\sqrt{-h}(x-ct)\right)\right). \tag{4.8}$$

(iii) When $\alpha_1 = 0$, $\alpha_2 < 0$, $\alpha_3 > 0$, corresponding to **Figure 2(8)**. There exist a center point $\left(-\frac{\alpha_3}{\alpha_2}, 0\right)$ on the *v-axis*. When $H\left(-\frac{\alpha_3}{\alpha_2}, 0\right) < h < 0$, the curves defined by $H(v,y) = h$ is a family of periodic orbits surrounding the center point $\left(-\frac{\alpha_3}{\alpha_2}, 0\right)$. From Equation (4.2), then we get

$$\sqrt{-h}\xi = \int_v^{\lambda_2} \sqrt{\frac{1}{(\lambda_2 - s)(s - \lambda_1)}} \mathrm{ds}, \tag{4.9}$$

where $\lambda_1 = \frac{\alpha_2 + \sqrt{h\alpha_3 + \alpha_2^2}}{h}$, $\lambda_2 = \frac{\alpha_2 - \sqrt{h\alpha_3 + \alpha_2^2}}{h}$.

From Equation (4.9), we get

$$v(\xi) = \frac{1}{2}(\lambda_2 - \lambda_1)\sin\left(\sqrt{-h}\xi\right) + \frac{1}{2}(\lambda_1 + \lambda_2), \tag{4.10}$$

and

$$u(x,t)=\ln\left(\frac{1}{2}(\lambda_2-\lambda_1)\sin\left(\sqrt{-h}(x-ct)\right)+\frac{1}{2}(\lambda_1+\lambda_2)\right). \tag{4.11}$$

(iv) When $\alpha_1<0$, $\alpha_2=0$, $\alpha_3=0$, corresponding to **Figure 2(10)**. There exist a saddle point $(0,0)$ on the *v-axis*. When $h>0$, there exist a family of homoclinic orbits corresponding to a family of bright solitons of Equation (2.4). From Equation (4.2), we obtain

$$\sqrt{-2\alpha_1}\xi=\int_v^{-\frac{h}{2\alpha_1}}\frac{1}{\sqrt{-s^3-\frac{h}{2\alpha_1}s^2}}\mathrm{d}s. \tag{4.12}$$

From Equation (4.12), we get the following parameter expressions for $v(\xi)$ and $u(x,t)$, as shown in **Figure 5** and **Figure 6**.

$$v(\xi)=-\frac{2h\mathrm{e}^{\frac{\sqrt{-2\alpha_1}}{2}\sqrt{-\frac{2h}{\alpha_1}}\xi}}{\alpha_1\left(1+\mathrm{e}^{\frac{\sqrt{-2\alpha_1}}{2}\sqrt{-\frac{2h}{\alpha_1}}\xi}\right)^2}, \tag{4.13}$$

and

$$u(x,t)=\ln\left(-\frac{2h\mathrm{e}^{\frac{\sqrt{-2\alpha_1}}{2}\sqrt{-\frac{2h}{\alpha_1}}(x-ct)}}{\alpha_1\left(1+\mathrm{e}^{\frac{\sqrt{-2\alpha_1}}{2}\sqrt{-\frac{2h}{\alpha_1}}(x-ct)}\right)^2}\right). \tag{4.14}$$

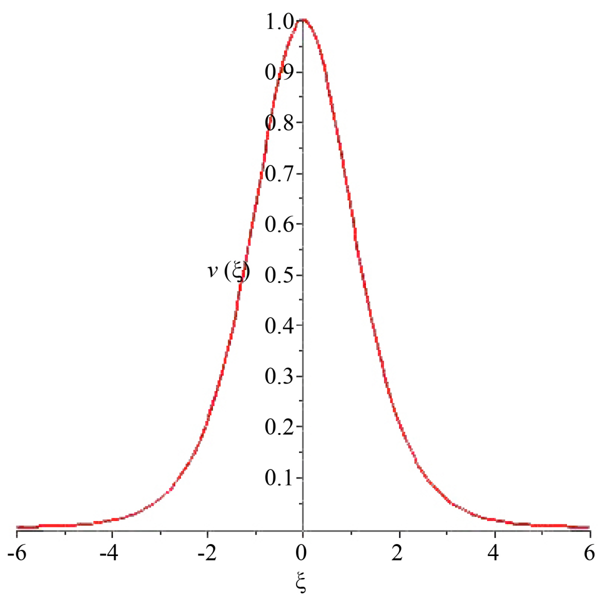

Figure 5. The 2D plot of (4.13).

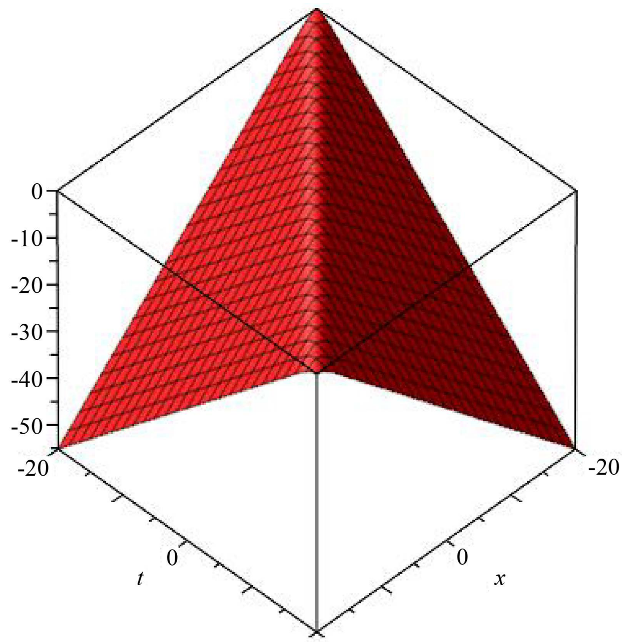

Figure 6. The 3D plot of (4.14).

(v) When $\alpha_1 < 0$, $\alpha_2 = 0$, $\alpha_3 > 0$ or $\alpha_1 < 0$, $\alpha_2 > 0$, $\frac{\alpha_3}{\alpha_2} > \sqrt{-\frac{4\alpha_2}{27\alpha_1}}$ or $\alpha_1 < 0$, $\alpha_2 > 0$, $\frac{\alpha_3}{\alpha_2} = \sqrt{-\frac{4\alpha_2}{27\alpha_1}}$ or $\alpha_1 < 0$, $\alpha_2 > 0$, $0 < \frac{\alpha_3}{\alpha_2} < \sqrt{-\frac{4\alpha_2}{27\alpha_1}}$ or $\alpha_1 < 0$, $\alpha_2 < 0$, $\alpha_3 > 0$, corresponding to **Figure 2(12)**, **Figure 2(21)**, **Figure 2(23)**, **Figure 2(25)**, **Figure 2(34)**, respectively. There exists a center equilibrium point $(v^*, 0)$ on the right of *y-axis*, respectively. When $h > H(v^*, 0)$, there exists a family of periodic orbits defined by $H(v, y) = h$, respectively. Especially, when $\alpha_1 < 0$, $\alpha_2 = 0$, $\alpha_3 > 0$, then $v^* = \sqrt[3]{-\frac{\alpha_3}{\alpha_1}}$. From Equation (4.2), we have

$$\begin{aligned}\sqrt{-2\alpha_1}\xi &= \int_v^{\lambda_3} \frac{1}{\sqrt{-v^3 - \frac{hv^2}{2\alpha_1} + \frac{v\alpha_2}{\alpha_1} + \frac{\alpha_3}{2\alpha_1}}} \mathrm{d}s \\ &= \int_v^{\lambda_3} \frac{1}{\sqrt{(\lambda_3 - s)(s - \lambda_2)(s - \lambda_1)}} \mathrm{d}s.\end{aligned} \tag{4.15}$$

where $\lambda_3 > \lambda_2 > \lambda_1$, and satisfies $\lambda_i^3 + \frac{h}{2\alpha_1}\lambda_i^2 - \frac{\alpha_2}{\alpha_1}\lambda_i - \frac{\alpha_3}{2\alpha_1} = 0$, $i = 1, 2, 3$.

From (4.15), we get the following solutions for $v(\xi)$ and $u(x,t)$, as shown in **Figure 7** and **Figure 8**.

$$v(\xi) = (\lambda_2 - \lambda_3) JacobiSN\left(\frac{1}{2}\sqrt{-2\alpha_1}\xi\sqrt{\lambda_3 - \lambda_1}, \sqrt{\frac{\lambda_3 - \lambda_2}{\lambda_3 - \lambda_1}}\right)^2 + \lambda_3, \tag{4.16}$$

and

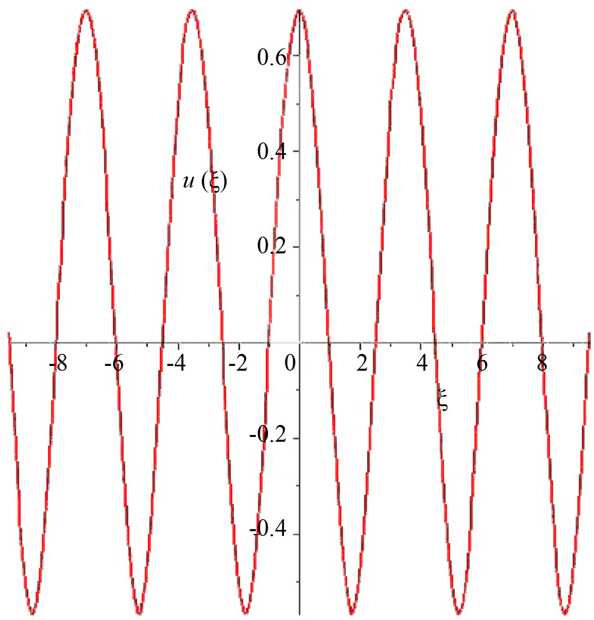

Figure 7. The 2D plot of (4.17).

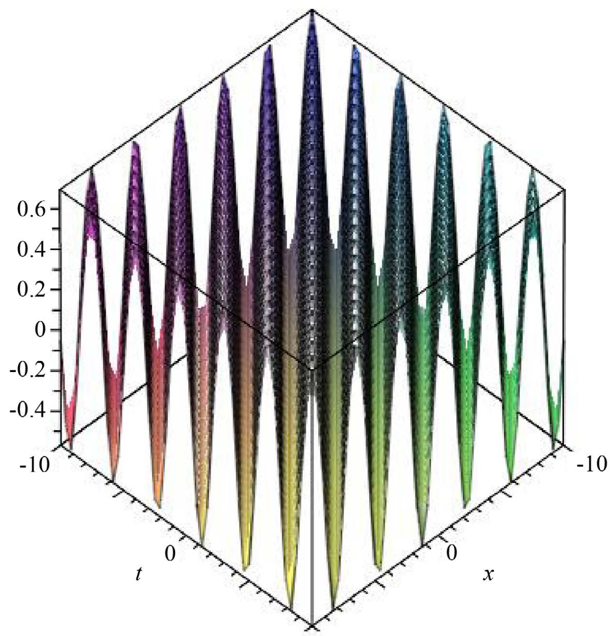

Figure 8. The 3D plot of (4.17).

$$u(x,t)=\ln\left((\lambda_2-\lambda_3)\,JacobiSN\left(\frac{\sqrt{2\alpha_1(\lambda_1-\lambda_3)}}{2}(x-ct),\sqrt{\frac{\lambda_3-\lambda_2}{\lambda_3-\lambda_1}}\right)^2+\lambda_3\right), \quad (4.17)$$

where $JacobiSN(\cdot,\cdot)$ is an elliptic integral of the first kind.

(vi) When $\alpha_1<0$, $\alpha_2<0$, $\alpha_3=0$, corresponding to **Figure 2(16)**. When $h\in(-\infty,+\infty)$, there exist a family of periodic orbits defined by $H(v,y)=h$. We obtain the parameter expressions for $v(\xi)$ and $u(x,t)$ as follows

$$v(\xi)=\lambda_2 JacobiCN\left(\frac{1}{2}\sqrt{-2\alpha_1}\xi\sqrt{\lambda_2-\lambda_1},\sqrt{\frac{\lambda_2}{\lambda_2-\lambda_1}}\right)^2, \tag{4.18}$$

and

$$u(x,t)=\ln\left(\lambda_2 JacobiCN\left(\frac{1}{2}\sqrt{-2\alpha_1}\sqrt{\lambda_2-\lambda_1}(x-ct),\sqrt{\frac{\lambda_2}{\lambda_2-\lambda_1}}\right)^2\right), \tag{4.19}$$

where $\lambda_1=\frac{-h+\sqrt{h^2+16\alpha_1\alpha_2}}{4\alpha_1}$, $\lambda_2=-\frac{h+\sqrt{h^2+16\alpha_1\alpha_2}}{4\alpha_1}$.

(vii) When $\alpha_1>0$, $\alpha_2<0$, $\alpha_3=0$, corresponding to Figure 2(17). There are two saddle points $(0,0)$ and $\left(\sqrt{-\frac{\alpha_2}{\alpha_1}},0\right)$, where $(0,0)$ is a degenerate saddle point.

(a) When $h=H\left(\sqrt{-\frac{\alpha_2}{\alpha_1}},0\right)$, there exists a homoclinic orbit connecting $(0,0)$ and $\left(\sqrt{-\frac{\alpha_2}{\alpha_1}},0\right)$. From Equation (4.2), we get

$$\sqrt{2\alpha_1}\xi=\int\frac{1}{\left(\sqrt{-\frac{\alpha_2}{\alpha_1}}-s\right)\sqrt{s}}\mathrm{ds}. \tag{4.20}$$

From Equation (4.20), we get the parameter expressions for $v(\xi)$ and $u(x,t)$ as follows

$$v(\xi)=1-\sqrt{-\frac{\alpha_2}{\alpha_1}}\tanh\left(\frac{1}{2}\sqrt{2}\sqrt{\alpha_1}\xi\sqrt[4]{-\frac{\alpha_2}{\alpha_1}}\right)^2, \tag{4.21}$$

and

$$u(x,t)=\ln\left(1-\sqrt{-\frac{\alpha_2}{\alpha_1}}\tanh\left(\frac{x-ct}{2}\sqrt{2}\sqrt{\alpha_1}\sqrt[4]{-\frac{\alpha_2}{\alpha_1}}\right)^2\right). \tag{4.22}$$

(b) When $h<H\left(\sqrt{-\frac{\alpha_2}{\alpha_1}},0\right)$, there exist a family of periodic orbits passing the saddle point $(0,0)$. The parameter expressions for $v(\xi)$ and $u(x,t)$ as follows

$$v(\xi)=\frac{\lambda_2\lambda_1 JacobiSN\left(\frac{\sqrt{2}}{2}\sqrt{\alpha_1}\xi\sqrt{\lambda_2},\sqrt{\frac{\lambda_1}{\lambda_2}}\right)^2-\lambda_2\lambda_1}{\lambda_2 JacobiSN\left(\frac{\sqrt{2}}{2}\sqrt{\alpha_1}\xi\sqrt{\lambda_2},\sqrt{\frac{\lambda_1}{\lambda_2}}\right)^2-\lambda_2}, \tag{4.23}$$

and

$$u(x,t)=\ln\left(\frac{\lambda_2\lambda_1 JacobiSN\left(\frac{\sqrt{2}(x-ct)}{2}\sqrt{\alpha_1}\sqrt{\lambda_2},\sqrt{\frac{\lambda_1}{\lambda_2}}\right)^2-\lambda_2\lambda_1}{\lambda_2 JacobiSN\left(\frac{\sqrt{2}(x-ct)}{2}\sqrt{\alpha_1}\sqrt{\lambda_2},\sqrt{\frac{\lambda_1}{\lambda_2}}\right)^2-\lambda_2}\right). \tag{4.24}$$

where $\lambda_1=-\frac{h+\sqrt{h^2+16\alpha_1\alpha_2}}{4\alpha_1}$, $\lambda_2=\frac{-h+\sqrt{h^2+16\alpha_1\alpha_2}}{4\alpha_1}$.

(viii) When $\alpha_1<0$, $\alpha_2>0$, $\alpha_3=0$, corresponding to **Figure 2(18)**. There exist a center point $\left(\sqrt{-\frac{\alpha_2}{\alpha_1}},0\right)$ on *v-axis*. When $h>H\left(\sqrt{-\frac{\alpha_2}{\alpha_1}},0\right)$, there exist a family of periodic orbits defined by $H(v,y)=h$. We obtain $v(\xi)$ and $u(x,t)$ as follows

$$v(\xi)=(\lambda_1-\lambda_2)\,JacobiSN\left(\frac{1}{2}\sqrt{-2\alpha_1}\xi\sqrt{\lambda_2},\sqrt{\frac{\lambda_2-\lambda_1}{\lambda_2}}\right)^2+\lambda_2, \tag{4.25}$$

and

$$u(x,t)=\ln\left((\lambda_1-\lambda_2)\,JacobiSN\left(\frac{\sqrt{-2\alpha_1\lambda_2}}{2}(x-ct),\sqrt{\frac{\lambda_2-\lambda_1}{\lambda_2}}\right)^2+\lambda_2\right), \tag{4.26}$$

where $\lambda_1=\frac{-h+\sqrt{h^2+16\alpha_1\alpha_2}}{4\alpha_1}$, $\lambda_2=-\frac{h+\sqrt{h^2+16\alpha_1\alpha_2}}{4\alpha_1}$.

(ix) When $\alpha_1<0$, $\alpha_2>0$, $-\sqrt{-\frac{4\alpha_2}{27\alpha_1}}<\frac{\alpha_3}{\alpha_2}<0$, corresponding to **Figure 2(27)**. There exist two saddle points $(v_1,0)$, $(v_2,0)$ and a center point $(v_3,0)$, where $v_1<0<v_2<v_3$.

(a) When $h=H(v_2,0)$, there exists a homoclinic orbit connecting the point $(v_2,0)$. From Equation (4.2), we have

$$\sqrt{-2\alpha_1}\xi=\int\frac{1}{\sqrt{-v^3-\frac{hv^2}{2\alpha_1}+\frac{v\alpha_2}{\alpha_1}+\frac{\alpha_3}{2\alpha_1}}}\mathrm{d}v=\int\frac{1}{(v-v_2)\sqrt{v_4-v}}\mathrm{d}v, \tag{4.27}$$

where $v_4>v_2$. From (4.27), we obtain

$$v(\xi)=v_4+(v_4-v_2)\tan\left(\frac{1}{2}\sqrt{-2\alpha_1}\sqrt{v_2-v_4}\xi\right)^2, \tag{4.28}$$

and

$$u(x,t)=\ln\left(v_4+(v_4-v_2)\tan\left(\frac{1}{2}\sqrt{2\alpha_1(v_4-v_2)}(x-ct)\right)^2\right). \tag{4.29}$$

(b) When $H(v_3,0)<h<H(v_2,0)$, there exists a family of periodic orbits defined by $H(v,y)=h$. The parameter expressions of $v(\xi)$ and $u(x,t)$ are the same as Equation (4.16) and Equation (4.17).

(x) When $\alpha_1>0$, $\alpha_2<0$, $-\sqrt{-\frac{4\alpha_2}{27\alpha_1}}<\frac{\alpha_3}{\alpha_2}<0$, corresponding to **Figure 2(28)**. There exist two center points $(v_1,0)$, $(v_2,0)$ and a saddle point $(v_3,0)$, where $v_1<0<v_2<v_3$.

(a) When $h=H(v_3,0)$, there exists a homoclinic orbit connecting the point $(v_3,0)$. From Equation (4.2), we have

$$\sqrt{2\alpha_1}\xi = \int \frac{1}{\sqrt{v^3 + \frac{hv^2}{2\alpha_1} - \frac{v\alpha_2}{\alpha_1} - \frac{\alpha_3}{2\alpha_1}}} \mathrm{d}v = \int \frac{1}{(v_3 - v)\sqrt{v - v_4}} \mathrm{d}v, \tag{4.30}$$

where $0 < v_4 < v_3$. From (4.30), we get $v(\xi)$ and $u(x,t)$, as shown in Figure 9 and Figure 10.

$$v(\xi) = v_4 + (v_4 - v_3)\tan\left(\frac{1}{2}\sqrt{2}\sqrt{\alpha_1}\xi\sqrt{v_4 - v_3}\right)^2, \tag{4.31}$$

and

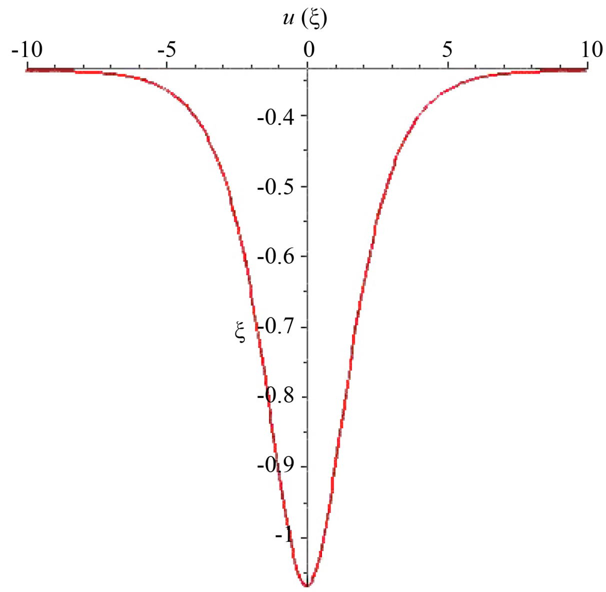

Figure 9. The 2D plot of (4.32).

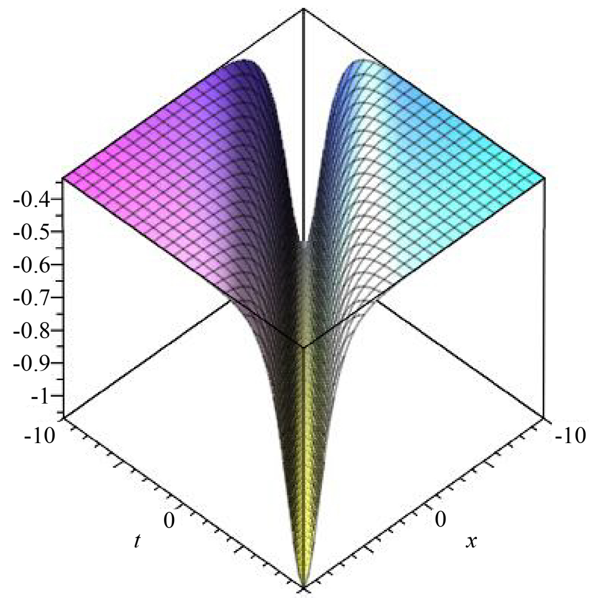

Figure 10. The 3D plot of (4.32).

$$u(x,t)=\ln\left(v_4+(v_4-v_3)\tan\left(\frac{1}{2}\sqrt{2}\sqrt{\alpha_1}\xi\sqrt{v_4-v_3}\right)^2\right), \tag{4.32}$$

where $v(\xi)$ is a bright soliton and $u(x,t)$ is a dark soliton.

(b) When $H(v_2,0)<h<H(v_3,0)$, there exists a family of periodic orbits defined by $H(v,y)=h$. From Equation (4.2), it follows

$$\sqrt{2\alpha_1}\xi=\int_v^{\lambda_2}\frac{1}{\sqrt{v^3+\frac{hv^2}{2\alpha_1}-\frac{v\alpha_2}{\alpha_1}-\frac{\alpha_3}{2\alpha_1}}}\mathrm{d}v=\int_v^{\lambda_2}\frac{1}{\sqrt{(\lambda_3-s)(\lambda_2-s)(s-\lambda_1)}}\mathrm{d}s. \tag{4.33}$$

where $\lambda_3>\lambda_2>\lambda_1$, and satisfies $\lambda_i^3+\frac{h}{2\alpha_1}\lambda_i^2-\frac{\alpha_2}{\alpha_1}\lambda_i-\frac{\alpha_3}{2\alpha_1}=0$, $i=1,2,3$.

From (4.33), then we get the periodic wave solutions as follows

$$v(\xi)=\frac{\lambda_3(\lambda_2-\lambda_1)JacobiSN\left(\frac{\sqrt{2\alpha_1(\lambda_3-\lambda_1)}}{2}\xi,\sqrt{\frac{\lambda_2-\lambda_1}{\lambda_3-\lambda_1}}\right)^2-\lambda_2(\lambda_3-\lambda_1)}{(\lambda_2-\lambda_1)JacobiSN\left(\frac{\sqrt{2\alpha_1(\lambda_3-\lambda_1)}}{2}\xi,\sqrt{\frac{\lambda_2-\lambda_1}{\lambda_3-\lambda_1}}\right)^2-\lambda_3+\lambda_1}, \tag{4.34}$$

and

$$u(x,t)=\ln\left(\frac{\lambda_3(\lambda_2-\lambda_1)JacobiSN\left(\frac{\sqrt{2\alpha_1(\lambda_3-\lambda_1)}}{2}(x-ct),\sqrt{\frac{\lambda_2-\lambda_1}{\lambda_3-\lambda_1}}\right)^2-\lambda_2(\lambda_3-\lambda_1)}{(\lambda_2-\lambda_1)JacobiSN\left(\frac{\sqrt{2\alpha_1(\lambda_3-\lambda_1)}}{2}(x-ct),\sqrt{\frac{\lambda_2-\lambda_1}{\lambda_3-\lambda_1}}\right)^2-\lambda_3+\lambda_1}\right). \tag{4.35}$$

5. Conclusion

To summarize, with the help of differential equation dynamical systems theory and methods, we obtain all bifurcation phase diagrams with directional fields. These directional fields can help us better grasp its dynamic behavior. By the same energy value of the Hamiltonian function corresponding to the same orbit, we get a lot of periodic wave solutions and bright soliton, dark soliton solutions.

Conflicts of Interest

The author declares no conflicts of interest regarding the publication of this paper.

References

[1] Kumar, D., Hosseini, K. and Samadani, F. (2017) The Sine-Gordon Expansion Method to Look for the Traveling Wave Solutions of the Tzitzéica Type Equations in Nonlinear Optics. *Optik*, **149**, 439-446. https://doi.org/10.1016/j.ijleo.2017.09.066

[2] Wazwaz, A. (2005) The Tanh Method: Solitons and Periodic Solutions for the

Dodd-Bullough-Mikhailov and the Tzitzéica-Dodd-Bullough Equations. *Chaos, Solitons & Fractals*, **25**, 55-63. https://doi.org/10.1016/j.chaos.2004.09.122

[3] Huber, A. (2008) A Note on a Class of Solitary-Like Solutions of the Tzitzéica Equation Generated by a Similarity Reduction. *Physica D: Nonlinear Phenomena*, **237**, 1079-1087. https://doi.org/10.1016/j.physd.2007.12.008

[4] Kaplan, M. and Hosseini, K. (2018) Investigation of Exact Solutions for the Tzitzéica Type Equations in Nonlinear Optics. *Optik*, **154**, 393-397. https://doi.org/10.1016/j.ijleo.2017.08.116

[5] Hosseini, K., Ayati, Z. and Ansari, R. (2017) New Exact Traveling Wave Solutions of the Tzitzéica Type Equations Using a Novel Exponential rational Function Method. *Optik*, **148**, 85-89. https://doi.org/10.1016/j.ijleo.2017.08.030

[6] Borisov, A., Zykov, S. and Pavlov, M. (2002) Tzitzéica Equation and Proliferation of Nonlinear Integrable Equations. *Theoretical and Mathematical Physics*, **131**, 550-557. https://doi.org/10.1023/A:1015162021255

[7] Ghanbari, B. and Rada, L. (2019) Solitary Wave Solutions to the Tzitzéica Type Equations Obtained by a New Efficient Approach. *Journal of Applied Analysis & Computation*, **9**, 568-589. https://doi.org/10.11948/2156-907X.20180103

[8] Zafar, A., Rezazadeh, H. and Bekir, A. (2021) The Simplest Equation Approach for Solving Non-Linear Tzitzéica Type Equations in Non-Linear Optics. *Modern Physics Letters B*, **35**, Article ID: 2150132. https://doi.org/10.1142/S0217984921501323

[9] Hosseini, K. and Ansari, R. (2018) New Exact Solutions of the Tzitzéica-Type Equations in Non-Linear Optics Using the Exp_a Function Method. *Journal of Modern Optics*, **65**, 847-851. https://doi.org/10.1080/09500340.2017.1407002

[10] Abazari, R. (2010) The $\left(\frac{G'}{G}\right)$-Expansion Method for Tzitzéica Type Nonlinear Evolution Equations. *Mathematical and Computer Modelling*, **52,** 1834-1845. https://doi.org/10.1016/j.mcm.2010.07.013

[11] Manafian, J. and Lakestani, M. (2016) Dispersive Dark Optical Soliton with Tzitzéica Type Nonlinear Evolution Equations Arising in Nonlinear Optics. *Optical and Quantum Electronics*, **48**, Article No. 116. https://doi.org/10.1007/s11082-016-0371-y

[12] Akbar, M., Abdullah, F. and Gepreel, K. (2022) Self-Controlled Wave Solutions to the Tzitzéica-Type Nonlinear Models in Mathematical Physics. *Results in Physics*, **36**, Article ID: 105451. https://doi.org/10.1016/j.rinp.2022.105451

[13] Babalic, C., Constantinescu, R. and Gerdjikov, V. (2015) On the Soliton Solutions of a Family of Tzitzéica Equations. *Journal of Geometry and Symmetry in Physics*, **37**, 1-24. https://doi.org/10.7546/jgsp-37-2015-1-24

[14] Zhou, J., Zhou, R. and Zhu, S. (2020) Peakon, Rational Function and Periodic Solutions for Tzitzéica-Dodd-Bullough Type Equations. *Chaos, Solitons & Fractals*, **14**, Article ID: 110419. https://doi.org/10.1016/j.chaos.2020.110419

[15] Conte, R., Musette, M. and Grundland, A. (1999) Bäcklund Transformation of Partial Differential Equations from the Painlevé-Gambier Classification. II. Tzitzéica Equation. *Journal of Mathematical Physics*, **40**, 2092-2106. https://doi.org/10.1063/1.532853

[16] Babalic, N., Constantinescu, R. and Gerdjikov, V. (2014) On Tzitzéica Equation and Spectral Properties of Related Lax Operators. *Balkan Journal of Geometry and Its Applications*, **19**, 11-22.

[17] Mirhosseini-Alizamini, S., Rezazadeh, H., Eslami, M., Mirzazadeh, M. and Kork-

maz, A. (2020) New Extended Direct Algebraic Method for the Tzitzéica Type Evolution Equations Arising in Nonlinear Optics. *Computational Methods for Differential Equations*, **8**, 28-53.

[18] Babalic, C., Constantinescu, R. and Gerdjikov, V. (2013) Two Soliton Solution of Tzitzéica Equation. *Physics AUC*, **23**, 36-41.

[19] Seadawy, A., Ali, A., Zahed, H. and Baleanu, D. (2020) The Klein-Fock-Gordon and Tzitzéica Dynamical Equations with Advanced Analytical Wave Solutions. *Results in Physics*, **19**, Article ID: 103565. https://doi.org/10.1016/j.rinp.2020.103565

[20] Arshed, S., Biswas, A., Abdelaty, M., Zhou, Q., Moshokoa, S. and Belic, M. (2018) Optical Soliton Perturbation for Gerdjikov-Ivanov Equation via Two Analytical Techniques. *Chinese Journal of Physics*, **56**, 2879-2886. https://doi.org/10.1016/j.cjph.2018.09.023

[21] Biswas, A., Mirzazadeh, M., Eslami, M., Milovic, D. and Belic, M. (2014) Solitons in Optical Metamaterials by Functional Variable Method and First Integral Approach. *Frequenz*, **68**, 525-530. https://doi.org/10.1515/freq-2014-0050

[22] Biswas, A. and Arshed, S. (2018) Application of Semi-Inverse Variational Principle to Cubic-Quartic Optical Solitons with Kerr and Power Law Nonlinearity. *Optik*, **172**, 847-850. https://doi.org/10.1016/j.ijleo.2018.07.105

[23] Khalique, C. and Biswas, A. (2009) A Lie Symmetry Approach to Nonlinear Schrödinger's Equation with Non-Kerr Law Nonlinearity. *Communications in Nonlinear Science and Numerical Simulation*, **14**, 4033-4040. https://doi.org/10.1016/j.cnsns.2009.02.024

[24] Wang, D. and Zhang, H. (2005) Further Improved F-Expansion Method and New Exact Solutions of Konopelchenko? CDubrovsky Equation, *Chaos Solitons & Fractals*, **25**, 601-610. https://doi.org/10.1016/j.chaos.2004.11.026

[25] Biswas, A., Ekici, M., Sonmezoglu, A. and Belic, M. (2019) Highly Dispersive Optical Solitons with Kerr Law Nonlinearity by F-Expansion. *Optik*, **181**, 1028-1038. https://doi.org/10.1016/j.ijleo.2018.12.164

[26] Zayed, E. (2011) A Note on the Modified Simple Equation Method Applied to Sharma-Tasso-Olver Equation. *Applied Mathematics & Computation*, **218**, 3962-3964. https://doi.org/10.1016/j.amc.2011.09.025

[27] Biswas, A., Yldrm, Y., Yaşar, E., Zhou, Q., Moshokoa, S. and Belic, M. (2018) Optical Soliton Solutions to Fokas-Lenells Equation Using Some Different Methods. *Optik*, **173**, 21-31. https://doi.org/10.1016/j.ijleo.2018.07.098

[28] Yan, Y., Liu, W., Zhou, Q. and Biswas, A. (2020) Dromion-Like Structures and Periodic Wave Solutions for Variable-Coefficients Complex Cubic-Quintic Ginzburg-Landau Equation Influenced by Higher-Order Effects and Nonlinear Gain. *Nonlinear Dynamics*, **99**, 1313-1319. https://doi.org/10.1007/s11071-019-05356-0

[29] Ben-Nun, M. and Martnez, T. (1998) Nonadiabatic Molecular Dynamics: Validation of the Multiple Spawning Method for a Multidimensional Problem. *The Journal of Chemical Physics*, **108**, 7244-7257. https://doi.org/10.1063/1.476142

[30] Girgis, L., Milovic, D., Konar, S., Yldrm, Y., Jafari, H. and Biswas, A. (2012) Optical Gaussons in Birefringent Fibers and DWDM Systems with Intermodal Dispersion. *Romanian Reports in Physics*, **64**, 663-671.

[31] Karpman, V. and Maslov, E. (1977) Perturbation Theory for Solitons. *Journal of Experimental and Theoretical Physics*, **73**, 537-559.

[32] Biswas, A. (2020) Optical Soliton Cooling with Polynomial Law of Nonlinear Refractive Index. *Journal of Optics*, **49**, 580-583.

https://doi.org/10.1007/s12596-020-00644-0

[33] Kudryashov, N. (2005) Simplest Equation Method to Look for Exact Solutions of Nonlinear Differential Equations. *Chaos, Solitons & Fractals*, **24**, 1217-1231. https://doi.org/10.1016/j.chaos.2004.09.109

[34] Mirzazadeh, M., Eslami, M., Vajargah, B. and Biswas, A. (2014) Optical Solitons and Optical Rogons of Generalized Resonant Dispersive Nonlinear Schrödinger's Equation with Power Law Nonlinearity. *Optik*, **125**, 4246-4256. https://doi.org/10.1016/j.ijleo.2014.04.014

[35] Yang, D., Lou, Q. and Zhang, J. (2022) Bifurcations and Exact Soliton Solutions for Generalized Dullin-Gottwald-Holm Equation with Cubic Power Law Nonlinearity. *The European Physical Journal Plus*, **137**, Article No. 240. https://doi.org/10.1140/epjp/s13360-022-02462-8

[36] Yang, D. (2021) Traveling Waves and Bifurcations for the (2+1)-Dimensional Heisenberg Ferromagnetic Spin Chain Equation. *Optik*, **248**, Article ID: 168058. https://doi.org/10.1016/j.ijleo.2021.168058

[37] Yang, D. and Zhang, J. (2022) The Soliton Wave Solutions and Bifurcations of the (2+1)-Dimensional Dissipative Long Wave Equation. *Journal of Nonlinear Mathematical Physics*, **29**, 659-677. https://doi.org/10.1007/s44198-022-00055-8

[38] Li, J. and Zhang, L. (2002) Bifurcations of Traveling Wave Solutions in Generalized Pochhammer-Chree Equation. *Chaos, Solitons & Fractals*, **14**, 581-593. https://doi.org/10.1016/S0960-0779(01)00248-X